Negative electron affinity material for increased ion detection sensitivity in electron multipliers

Toby Shanley, Wayne Sheils

ETP Electron Multipliers, 8 Martha St., Clyde, New South Wales, AUSTRALIA, 2142. Email contact: wsheils@etp-ms.com

Introduction

The Poisson distribution of emitted electrons from an ion-electron conversion process is the primary determining factor of the shape of the pulse height distribution (PHD) from an electron multiplier. This distribution also places a fundamental limit on the detection efficiency. The mean of the Poisson distribution of the electron emission is referred to as the secondary electron emission (SEE) yield.

We have used boron-doped diamond (BDD) as ion conversion, and next-stage dynodes, in electron multipliers (ETP MagneTOF® & HED multipliers, see Figure 1.) to compare the gains, pulse height distributions and plateau curves with unmodified detectors. The results demonstrate a large gain increase and a profoundly improved pulse height distribution.

Design Methods and Concepts

The boron doped diamond (BDD) was grown from seed nanodiamonds dispersed on a Mo substrate using Microwave plasma Assisted Chemical Vapour Deposition (MACVD). The polycrystalline film was composed of grains ~1-10 um in size, and the surface was terminated with hydrogen immediately after growth. The hydrogen termination on diamond induces a negative electron affinity, which allows electrons in the conduction band to freely escape the surface, significantly enhancing the escape depth of secondary electrons generated by ion or electron impact.

Of interest in HED detectors is the effect of the BDD as an ion-electron conversion dynode (CD), and as the next-stage dynode. Herein, a standard HED detector (HED=stainless, Dy1=Al_2O_3) is compared with an identical detector using BDD for the HED, as well as the following dynode (Dy1).

In the TOF detector tests, a standard ETP MagneTOF® (MagC) detector with Al_2O_3 on both the conversion dynode (CD) and Dy 1 is compared with a MagC modified by placing BDD inserts onto these dynodes.

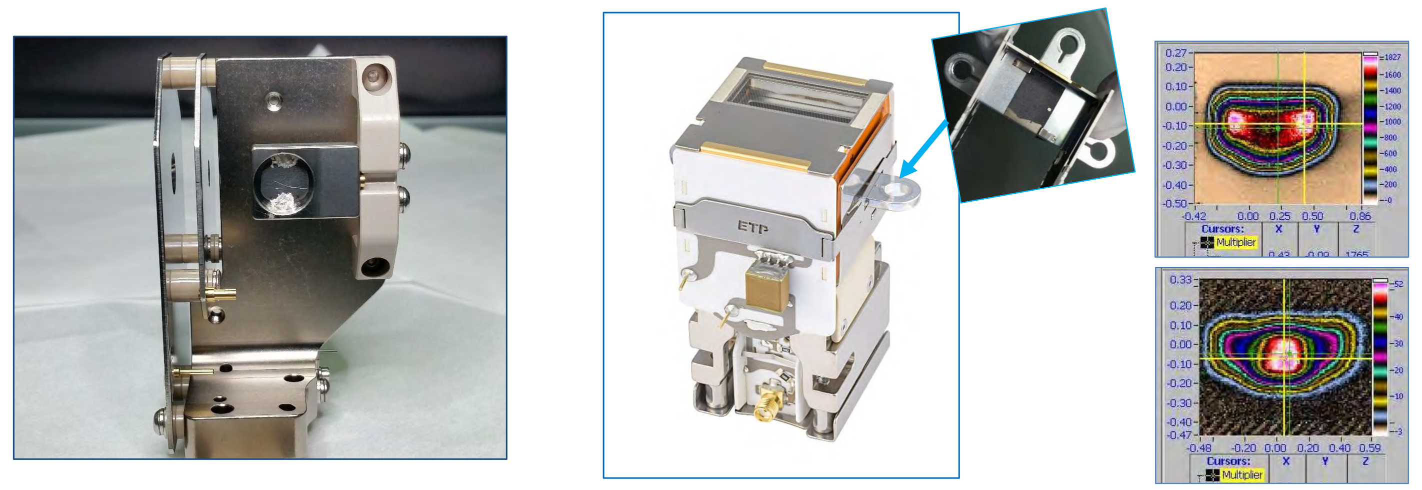

Figure 1.
BDD pieces inserted into HED detector (left) , TOF detector (middle).
The presence of the BDD on the TOF CD is evident from the aperture scans of the TOF detectors: standard MagC (top right), MagC with BDD insert (bottom right).

Preliminary Data

Gain

The effect on the gain of introducing BDD into detectors is shown in Figure 2.

In the HED detector, the gain boost provided by using BDD as the HED (instead of stainless steel) was a factor of ~ 5.8 at HV=1400V (HED = 10 kV). The gain boost from using BDD in the Dy1 position (instead of Al_2O_3) is also, coincidentally, ~ 5.8.

In the TOF detector, the combined gain enhancement provided by using BDD (instead of Al_2O_3) on both the CD and Dy1 was a factor of ~ 6.0 at HV=1900V.

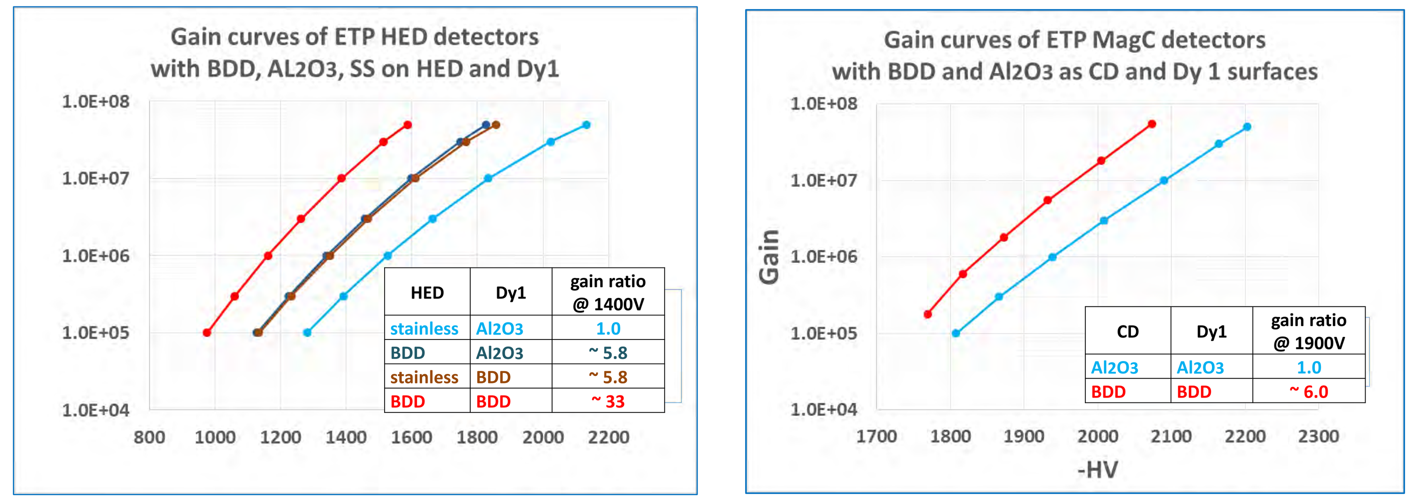

Figure 2. Gain curves of HED detectors (left) and TOF detectors (right).

Pulse Height Distributions – detection efficiency

The shape of the PHD from a detector depends strongly on the SEE yield of the initial ion conversion. Higher SEE yields lead to narrower PHDs, and indicate fewer detection losses. For SEE distributions with low mean values, there is a significant probability that zero electrons will be emitted when an ion is incident on the conversion surface.

The 'resolution' of a PHD is defined as the FWHM of the distribution divided by its mean. Figure 3.a).

The resolution of a PHD is independent of the gain of a detector. Figure 3.b).

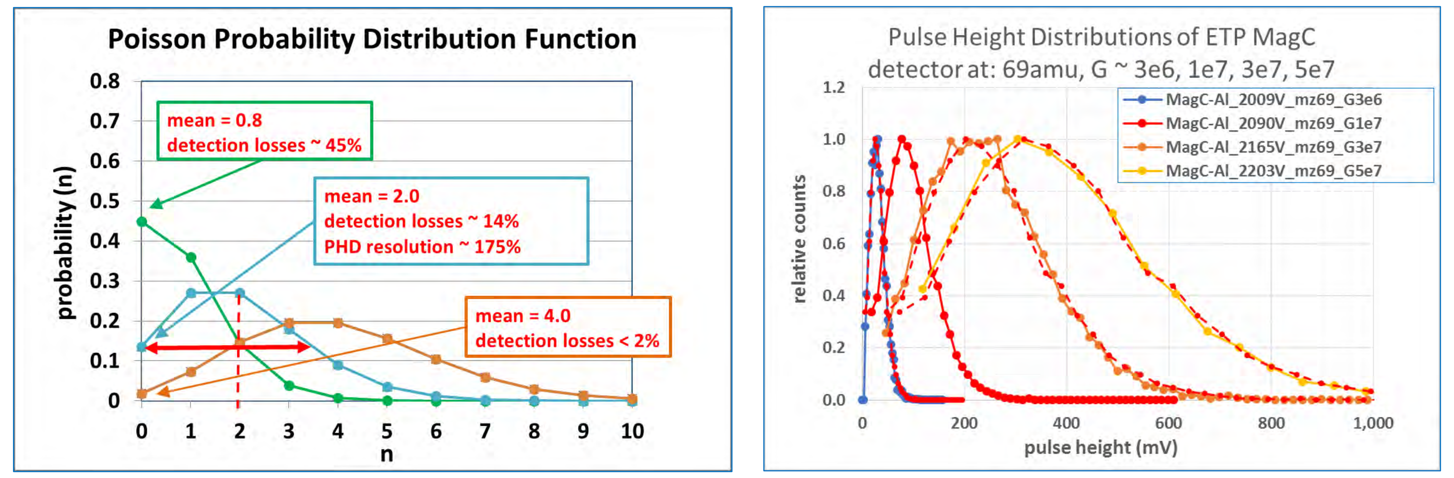

Figure 3.a) (left) Poisson distributions with means of 0.8, 2.0 and 4.0.
Figure 3.b) (right) PHDs from an ETP MagneTOF® detector at different gains. The G1e7 curve has been scaled (red dashed lines) to compare with the PHDs at the other gains, showing that the 'resolution' of the PHD is independent of gain.

PHDs in HED detector

The dramatic effects of the increased SEE yield on the PHDs of an HED detector are shown in Figure 4. The four PHDs have been collected at the same multiplier gain, but their resolutions are very different. In these data, ions of air impacted the HED at 10 keV.

When the HED surface is BDD, the full width of the PHD is clearly seen in the data, indicating a high SEE yield and a high ion detection efficiency.

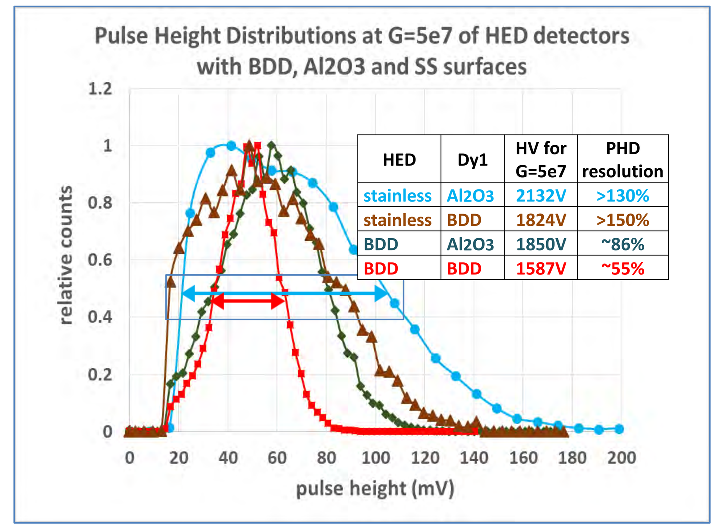

Figure 4. PHDs of 10 kV HED detector with BDD, Al_2O_3 and steel surfaces.

When the HED surface is stainless steel, the distribution of low-level pulses of the PHD has been truncated by the trigger level of the oscilloscope. This truncation by the trigger corresponds to losses within the detection system. Those pulses falling below the trigger could be detected if the gain of the multiplier was increased.

On the other hand, the resolutions of the PHDs from the stainless HEDs show that they originate from a lower SEE yield in the ion conversion process, indicating inherently greater statistical losses. These fundamental 'Poisson' losses cannot be regained by increasing the gain of the detector.

Notably, the increased detection efficiency obtained with the BDD HED is achieved with a dramatically lower multiplier HV, leading to a longer life for the detector. In essence, the increased yield from the ion conversion is allowing the rest of the multiplier to operate at a lower gain.

PHDs in TOF detector

In Figures 5. a)-c), the PHDs of a standard MagC detector (CD= Al_2O_3, Dy1= Al_2O_3) are compared with PHDs from an identical MagC but with CD=BDD, Dy1=BDD.

In Figure 5. a) air ions impact the CD with the energy provided by –HV (~2100V). Comparing with the data in Fig. 4, several features can be noted:

- the PHD of the Al_2O_3 detector is again truncated on the side of the low-level pulses, and is much broader than the PHD for the BDD detector

- the resolution of the BDD PHD is ~92% for the TOF detector cf. ~55% for the BDD HED detector. This reflects the lower SEE yield from the first two interactions due to the lower energies involved.

- the pulse heights for the MagC detector are ~10x higher than for the HED detector, due to their 10x narrower pulse width (~0.5ns cf. ~5ns)

Figure 5. b) shows PHDs collected in a TOF system, where the ions (m/z = 69, 285) impacted the CD with an energy of ~5 keV. The Al_2O_3 and BDD PHDs in this figure have been collected at different gains. At first glance, the PHDs appear to be very similar. In Fig. 5c, the BDD PHDs have been scaled down to compare with those from the Al_2O_3 MagC. The improved resolutions of the BDD PHDs are evident in this figure, indicating higher SEE yields from the ion-electron conversion.

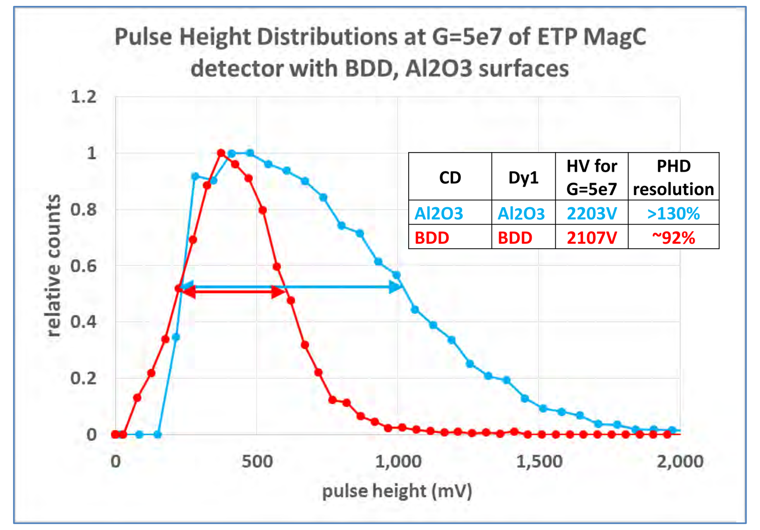

Figure 5.a) PHDs of TOF detectors with BDD and Al_2O_3 surfaces. Ion energy ~2.1keV.

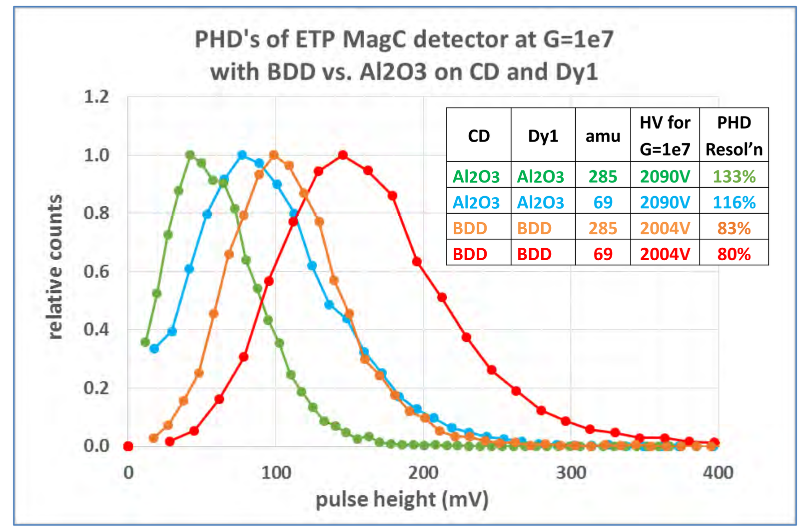

Figure 5.b) PHDs of TOF detector with BDD and Al_2O_3 surfaces. Ion energy = 5 keV.

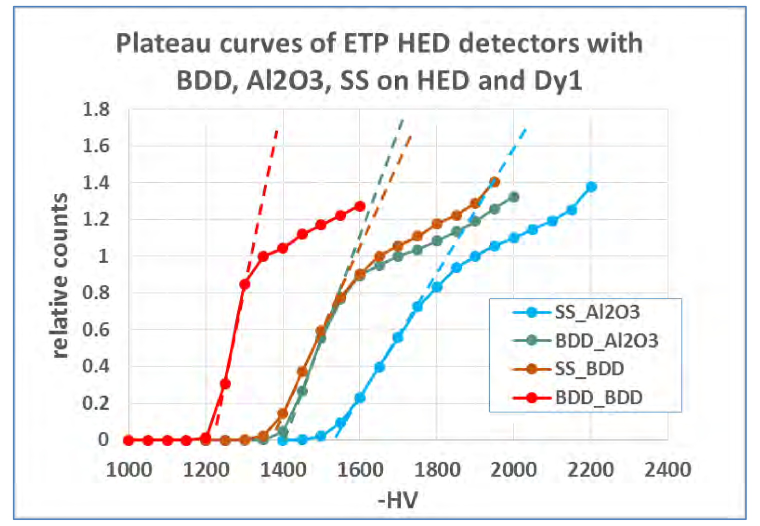

Figure 6. Plateau curves of HED detector with BDD and Al_2O_3 surfaces. Ion energy ~2.1keV.

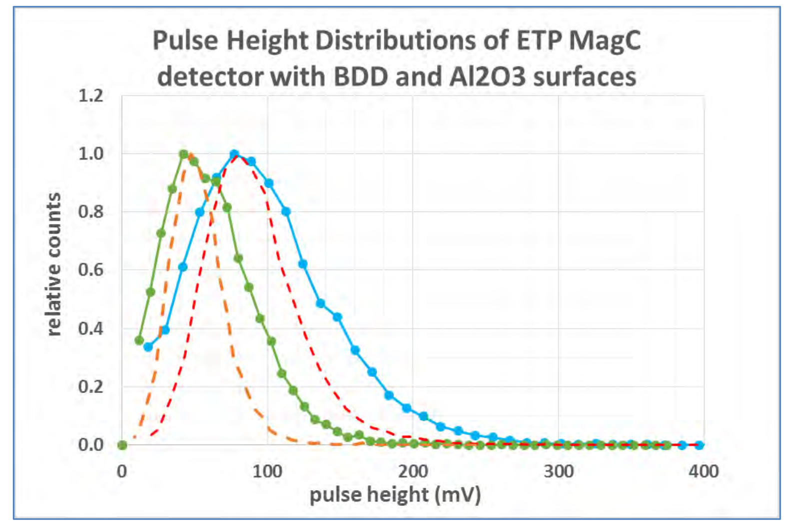

Figure 5.c) Al_2O_3 PHDs of Figure 5.b) with scaled BDD PHDs for comparison.

Plateau curves

Plateau curves collected from the HED detectors are shown in Figure 6.

The knees of the plateaus are much sharper for the BDD detectors, and occur at much lower voltages.

The slope of the rising edge of a plateau curve contributes to the sharpness of its knee. This slope is derived from the shape of the high-pulse side of the PHD, which is reflected in the resolution measurement of the PHD.

Conclusions

The inclusion of BDD in HED and TOF detectors has produced greatly improved pulse height distributions that have impacted strongly on the operating performance of the detectors. Greater detection efficiencies at lower operating gains have been demonstrated.

Acknowledgements

This work was performed in part at the Melbourne Centre for Nanofabrication (MCN) in the Victorian Node of the Australian National Fabrication Facility (ANFF)